

# Polyethyleneimine-Modified Graphene Oxide as Novel Antibacterial Agent and Its Synergistic Effect with Daptomycin for Methicillin-Resistant *Staphylococcus Aureus*

Zetan Fan,<sup>†</sup> Hiu Laam Po,<sup>‡</sup> Ka Kit Wong,<sup>†</sup> Sheng Chen,<sup>‡</sup> Shu Ping Lau<sup>†,\*</sup>.

<sup>†</sup>Department of Applied Physics, The Hong Kong Polytechnic University, Hong Kong, China

<sup>‡</sup>Department of Applied Biology and Chemical Technology, The Hong Kong Polytechnic University, Hong Kong, China

ABSTRACT: Aqueous dispersion of polyethyleneimine-modified graphene oxide (PEI-GO) was prepared *via* a one-step synthesis through the epoxy ring opening reaction. PEI-GO exhibited the bacterial growth inhibition activity on methicillin-resistant *Staphylococcus aureus* (MRSA) with the minimum inhibitory concentration as low as 8  $\mu\text{g/mL}$ . Time-kill curves assay and SYTOX Green assay showed the antibacterial activity and the bacteria cell membrane permeability of PEI-GO, respectively. Most importantly, when employing PEI-GO at 1-2  $\mu\text{g/mL}$ , a synergistic effect with daptomycin to resensitize daptomycin-resistant MRSA was revealed. Synergistic effect between PEI-GO and daptomycin provides a possible way to increase bacterial killing and reduce the development of daptomycin resistance. The antibacterial activity of the PEI-GO is attributed to the damaged cell membrane caused by the sharp edge and chain structure of the PEI-GO nanosheets as well as the high density of amine groups presented in the PEI chains. Our results indicate that PEI-GO dispersion has a great potential for clinical pathogenic bacteria treatment.

KEYWORDS: Graphene oxide, Polyethyleneimine, Antibacterial, Synergistic effect, Methicillin-Resistant *Staphylococcus Aureus*

## INTRODUCTION

The rapid emergence of drug-resistant bacteria<sup>1-3</sup> has posed a global public health problem. It has ignited great interest in the novel strategies for combating antibiotic resistance. Infections caused by drug-resistant bacteria lead to dramatically increasing in death rate, morbidity, and expenditure regarding to the treatments.<sup>4</sup> According to a recent report, approximately 700,000 people are dead from drug-resistant bacteria each year, and the number will reach to 10 million by 2050 unless drastic action is taken.<sup>5</sup> With the rising threat of drug-resistant bacteria, it is of great urgency to explore new antibiotic agents as well as strategy which will be effective to oppose drug-resistant bacteria.

A relatively new antibiotic agent called Daptomycin has been adopted to treat multidrug-resistant Gram-positive bacteria, such as methicillin-resistant *Staphylococcus aureus* (MRSA).<sup>6-8</sup> Steenbergen *et al.* proposed an antibacterial mechanism of daptomycin, which involved the insertion of lipophilic tail of daptomycin into the cell membrane, then led to rapid depolarization of membrane and efflux of potassium ions.<sup>9</sup> However, more and more studies have reported the daptomycin resistance in association with clinical treatment failures in MRSA infections.<sup>10-12</sup> In order to minimize the emergence of daptomycin resistance, combinatorial therapy of using daptomycin with other reagents has been proposed. Most of the additional reagents are organic antibiotics,<sup>13-15</sup> and silver nanoparticles<sup>16</sup>, which may have the toxicity towards mammal cells.

Recently, carbon nanomaterials, including carbon nanotubes (CNTs)<sup>17-18</sup>, graphene oxide (GO) and reduced graphene oxide (rGO)<sup>19-21</sup>, have been demonstrated to show promising antibacterial

activity and excellent biocompatibility to mammal cells. It was found that carbon nanomaterials could cause both physical and chemical damages to bacteria. Vecitis *et al.* proposed a three-step single-walled CNTs antibacterial mechanism involving initial bacteria contact, cell membrane perturbation as well as electronic structure-dependent bacterial oxidation.<sup>22</sup> Liu *et al.* proposed an antibacterial mechanism of GO-based materials caused by membrane and oxidation stress.<sup>23</sup> The interaction between the bacterial cell and the sharp GO nanosheets led to the membrane stress and bacteria oxidation.<sup>23</sup> Pham *et al.* proved experimentally and theoretically that the density of graphene edges was the principal parameter that contributed to the antibacterial activity. They found the pores formed in the bacterial cell walls, which led to the imbalance of osmotic pressure and the bacteria death.<sup>24</sup> However, the antibacterial effect of the carbon nanomaterials would only be effective with high concentration and prolonged exposure time. It was demonstrated that GO nanowalls with a concentration of 1 mg/mL could kill 74% of *S. aureus* cell in 1 h.<sup>20</sup> The bacterial viability of *E. coli* cell could decrease to 0.5% when the suspension was exposed to GO for 3 h with a concentration of 200 µg/mL.<sup>21</sup> The high dosage and long exposure time are not desirable and limit the applicability of these nanomaterials for antibacterial agents. The development of new carbon nanomaterials with potent antibacterial performance is urgently needed.

One of the important characteristics for carbon nanomaterials is their easy chemical modification due to the carboxyl, epoxy and hydroxyl groups on their surfaces. They can be modified with micromolecules, biomacromolecules, polymers and inorganic nanomaterials by covalent or non-covalent bonds.<sup>25-27</sup> Polyethyleneimine (PEI) is a weakly alkaline aliphatic polymer with the existence of high-density primary, secondary and tertiary amine groups. The amine groups can be protonated easily. PEI has been widely used to enhance the antibacterial

activities of antibiotics due to its excellent biocompatibility and strong membrane-permeabilizing effect.<sup>28-30</sup> Furthermore, PEI can be covalently bonded with GO through the reaction between the amine groups on PEI and the oxygen functional groups on the surface of GO.<sup>31</sup> Huang *et al.* prepared a new drug delivery system by cross linking PEI on a GO film.<sup>32</sup> Compared with the original GO film, the stability of the PEI cross-linked film was significantly improved and thus exhibited an enhanced antibacterial effect.<sup>32</sup> It has also been reported that PEI-GO incorporated polyurethane film exhibited desirable antibacterial property, which was mainly attributed to the relative high density of amine groups presented in the PEI chains.<sup>33</sup> The above literature mainly focused on the study of antibacterial ability of GO-based films. However, the carbon nanomaterials-PEI hybrid aqueous dispersion with drug-resistant antibacterial behavior has not been explored. Compared with film, aqueous system is more suitable for biological applications (such as cell, animal models) and in-depth study. The aggregation of carbon nanomaterials usually exists through  $\pi$ - $\pi$  stacking in the aquatic systems, which has an important impact on the interaction between nanomaterials and bacteria. It was reported that GO dispersions exhibited better antibacterial activity than rGO aggregates since bacteria were wrapped by a thin layer of GO while embedded in large rGO aggregates.<sup>13</sup> Therefore it calls necessity to improve the water dispersity of carbon-based nanomaterials.

In this study, polyethyleneimine-modified graphene oxide (PEI-GO) aqueous dispersion *via* a one-step synthesis was prepared through the epoxy ring opening reaction at room temperature. Branched amine-group-rich PEI was used to simultaneously reduce and functionalize GO. The resultant PEI-GO aqueous dispersion is stable without precipitation even after one-week of storage at ambient conditions. PEI-GO exhibited bacterial growth inhibition activity on MRSA with MIC as low as 8  $\mu\text{g/mL}$ . Furthermore, time-kill curves assay showed the bacterial killing

ability of PEI-GO. SYTOX Green assay illustrated the bacteria cell membrane permeability of PEI-GO. Most importantly, when employing PEI-GO at 1-2  $\mu\text{g/mL}$ , a synergistic effect with daptomycin to resensitize daptomycin-resistant MRSA was revealed. The synergistic effect between PEI-GO and daptomycin provides promising hopes for reducing the development of daptomycin resistance and increasing bacteria killing power as compared with daptomycin monotherapy. Our results indicate that PEI-GO dispersion has a great potential for clinical pathogenic bacteria treatment.

## MATERIALS and METHODS

**Materials.** Graphite powder was bought from Asbury Carbons (USA). Sulfuric acid ( $\text{H}_2\text{SO}_4$ , 98 wt%), hydrogen peroxide ( $\text{H}_2\text{O}_2$ , 30 wt%), hydrochloric acid (HCl, 10 vol%), sodium nitrate ( $\text{NaNO}_3$ ) and potassium permanganate ( $\text{KMnO}_4$ ) were purchased from Sigma-Aldrich (USA). Branched polyethyleneimine (PEI) with number-average-molecular weight ( $M_n$ ) of 10000  $\text{kg mol}^{-1}$  was purchased from Sigma-Aldrich (USA). Ethanol (ACS grade, 99.9 wt%) was obtained from Anaqua (Hong Kong).

**Characterizations.** Scanning electron microscopy (SEM) was performed on JSM-633 $\beta$ F operating at 10 kV. Atomic force microscopy (AFM) (Digital Instruments Nanoscope IV) operating in the tapping mode was used to measure the height of the materials. X-ray diffraction (XRD) was obtained using Rigaku SmartLab X-ray diffractometer (Cu  $K\alpha$  radiation  $\lambda = 1.54056 \text{ \AA}$ ) operating at 45 kV and 200 mA. The Fourier transform infrared spectroscopy (FTIR) spectra were carried out with Bruker ALPHA FTIR spectrometer and the resolution is  $4 \text{ cm}^{-1}$ . The X-ray photoemission spectroscopy (XPS) measurements were performed on an AXIS Ultra DLD spectrometer equipped with a 150 W monochromatic Al  $K\alpha$  X-ray source (1486.6 eV). The Raman spectra were recorded on a LabRAM HR 800 Raman spectrometer with 488 nm

excitation. The UV-*vis* absorption spectra were measured on a Shimadzu UV-2550 spectrometer. Microscopic measurements were performed by Leica TCS SP8 MP.

**GO preparation.** GO was prepared by the modified Hummers' method<sup>34-35</sup>. 23 mL of 98% H<sub>2</sub>SO<sub>4</sub> was firstly added to the mixture of 1.0 g graphite powder and 0.5 g NaNO<sub>3</sub>. The mixture was cooled to 4 °C using an ice bath and stirred for 1 h. Add 3.0 g KMnO<sub>4</sub> to the mixture. Keep the reaction temperature at 5 °C and stir for 2 h. Then increase the temperature to 35 °C and stir for 30 min. Add 80 mL DI water to the reaction and slowly increase the temperature to 90 °C and react for 30 min. Then the reaction was cooled and followed by adding 60 mL DI water and 15 mL 30 wt% H<sub>2</sub>O<sub>2</sub> and stirred for 15 min. At last, 40 mL 10 vol% HCl was added and stirred for 10 min to end the reaction. After the reaction, the powder was obtained through centrifugation, washing with DI water and drying in a vacuum oven at 60 °C overnight.

**Modification of GO with PEI.** The GO (10 mg) was dispersed in 5 mL ethanol to form a stable suspension. Then 20 mg of PEI was added and mixed with the as prepared GO solution. The mixture was stirred for 24 h at room temperature. At last, the solid product, denoted as PEI-GO, was obtained through centrifugation, washing with DI water and drying in an oven.

**MIC test.** Susceptibility to PEI-GO was performed on *S. aureus* and *E. coli* strains by the standard broth dilution method according to the Clinical and Laboratory Standards Institute (CLSI)<sup>36-37</sup> and MICs were obtained by CLSI guideline<sup>38</sup>.

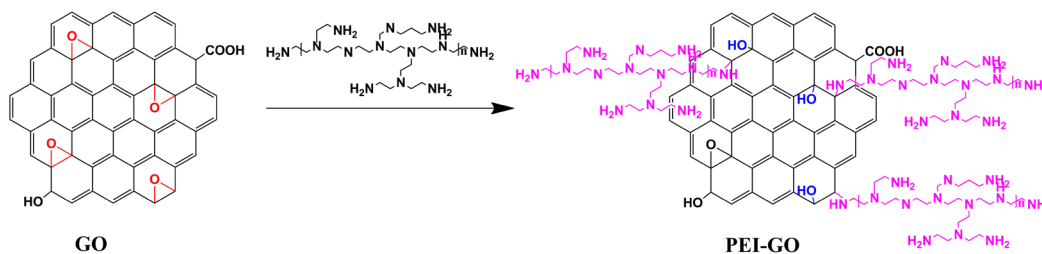
**Time-kill curves assay.** The *S. aureus* strain ATCC29213 was cultured overnight and was diluted 1:100 in Mueller-Hinton Broth and incubated at 37 °C with aeration at until OD<sub>600</sub> of 0.3. Bacteria were then treated with PEI-GO at different concentrations (64 and 128 µg/mL) at 37 °C and 250 r.p.m. At intervals, colony counts were performed.

**SYTOX Green assay.** The *S. aureus* strain ATCC29213 was cultured overnight and diluted 1:100 in MHB and incubated at 37 °C with aeration until OD<sub>600</sub> of 0.3. Bacteria were then treated with PEI-GO at different concentrations (16, 32 and 64 µg/mL) at 37 °C and 250 r.p.m. After 30 min, colony counts were performed and aliquots were removed, washed three times with sterile saline. 200 µL of bacteria suspension were incubated with 1 µM SYTOX Green for 10 min at room temperature. Fluorescence was measured by CLARIOstar microplate reader at 523±5 nm upon excitation at 504±5 nm. Microscopic measurements of membrane permeability were performed similarly as described above while 1mL of cell pellet was used instead. Fluorescence was measured by Leica TCS SP8 MP at 523±20 nm upon excitation at 504±20 nm. The signals were quantified by the LasX.

## RESULTS AND DISCUSSION

### Synthesis and characterization of PEI-GO

GO was firstly prepared by a modified Hummers' method, which is a relative fast and convenient method to produce GO with a relative high oxygen concentration. Then PEI was covalently linked to GO through the epoxy ring opening reaction under room temperature. As illustrated in Scheme 1, the reaction between the epoxy groups on GO and amine groups on PEI results in the formation of hydroxyl groups and PEI grafted on GO *via* C-N bond. Compared with GO aqueous dispersion, the resultant PEI-GO is stable without precipitation even after one-week of storage at ambient conditions (Figure S1), which is essential for biological applications.



**Scheme 1.** Schematic illustration of PEI-GO synthesis.

Aqueous dispersions of the GO and PEI-GO were then dropped onto silicon wafers, and SEM images were taken randomly. Figures 1a and e show the SEM images of the GO and PEI-GO. Image J software was used to determine the size distribution of the GO and PEI-GO samples. After PEI functionalization, the lateral size of GO decreases from 2.7  $\mu\text{m}$  (Figure 1b) to 0.3  $\mu\text{m}$  (Figure 1f). Figures 1c and g show AFM images of the GO and PEI-GO. The thickness of the PEI-GO is around 1 nm (Figure 1h), lower than the GO (Figure 1d), indicating the GO sheets with single layer are formed, which is probably due to the insertion of PEI into the GO layers.

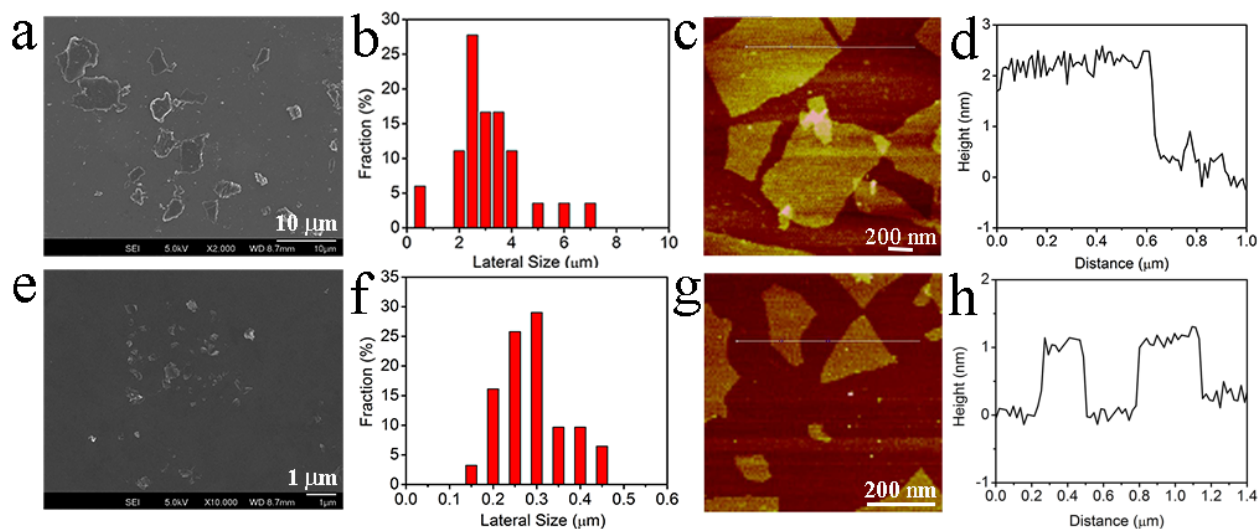


**Figure 1.** Representative SEM images by drying (a) GO and (e) PEI-GO dispersions on clean silicon wafers. Lateral size distributions of (b) GO and (f) PEI-GO. The size distribution was



obtained by measuring at least 100 particles for each sample. AFM images of (c) GO and (g) PEI-GO on clean silicon wafers and (e, f) the corresponding height profiles of the AFM images.

The UV-*vis* spectrum of GO (Figure 2a) shows an absorption band at 270 nm with a shoulder band at 320 nm, which are respectively attributed to  $\pi$ - $\pi^*$  transitions (C=C bonds) and n- $\pi^*$  transitions (C=O bonds). The PEI-GO UV-*vis* spectrum reveals PEI peak, which has a sharp absorption increase near 200 nm, superimposing with the absorption curve of GO, suggesting the successful conjunction of PEI onto GO. The XRD patterns of GO as well as PEI-GO are showed in Figure S2a. The XRD curve of GO exhibits a sharp diffraction peak at  $11.7^\circ$  and a typical blunt peak in the range of  $20$ - $30^\circ$ , indicating graphite has been completely converted into GO.<sup>39</sup> In the PEI-GO curve, the peak at  $11.7^\circ$  disappeared, indicating that the aggregation of GO sheets is partially prevented by PEI conjunction.<sup>40</sup> Raman spectra of GO and PEI-GO (Figure S2b) both exhibit G band at  $1592\text{ cm}^{-1}$  and D band at  $1340\text{ cm}^{-1}$ , corresponding to  $\text{sp}^2$  carbon domains and disordered structural defects respectively.

We firstly used FTIR to identify the reaction between PEI and GO. Figure 2b shows the FTIR spectra of GO, PEI and PEI-GO. Comparing with the individual GO and PEI, the peak of PEI-GO exhibits the typical signal of C-N stretch ( $1462\text{ cm}^{-1}$ ) and weak signal of N-H band ( $760\text{ cm}^{-1}$ ). At the same time, the C-O-C peak at  $1041\text{ cm}^{-1}$  became weaker. This result proves that the PEI is successfully modified on the GO by the reaction between C-O-C groups on the GO and the amine groups on the PEI.

We further analyzed the chemical bonding of the PEI-GO using XPS. As shown in Figure 2c, the N peak appeared in the XPS spectrum of PEI-GO clearly indicates the incorporation of PEI onto GO. The oxygen content in GO is estimated to be 28 at%, whereas the percentage of oxygen is decreased to 12 at% after PEI modification (Table S1). High-resolution C1s spectra of

the GO (Figure 2d) can be fitted into four fitted curves which are corresponding to  $sp^2$  C (284.5 eV),  $sp^3$  C (285.2 eV), C-O (286.5 eV), and O=C-O (288.5 eV), respectively. The appearance of the C-N peak at 286.0 eV in the C1s spectrum of the PEI-GO (Figure 2e) confirms that PEI chains are covalently linked to GO. The N1s spectrum of PEI-GO can be fitted into two components: one at 399.0 eV representing the C-N peak, the other at 400.8 eV corresponding to the partial protonation of C-N bond (Figure 2f).

We assume that the amine groups on PEI mainly reacted with the epoxy groups (C-O-C) on GO surface and results in the formation of hydroxyl groups and PEI grafted on the surface of GO via C-N bond as shown in Scheme 1. If C-O-C completely reacts with PEI, the number of containing C-O will be reduced by half after the reaction. At the same time, the number of COOH on the surface should not change before and after the reaction. Therefore, we could use the peak area ratio of C-O-C to COOH to estimate the amount of C-O-C consumed during the reaction. From the XPS C1s spectrum of GO (Figure 2d), the peak area ratio of C-O-C to COOH was 7.8. After the reaction with PEI, this peak area ratio changed to 3.5, which was about half of the previous ratio. This result indicates most C-O-C on GO has been grafted with amine groups on PEI.

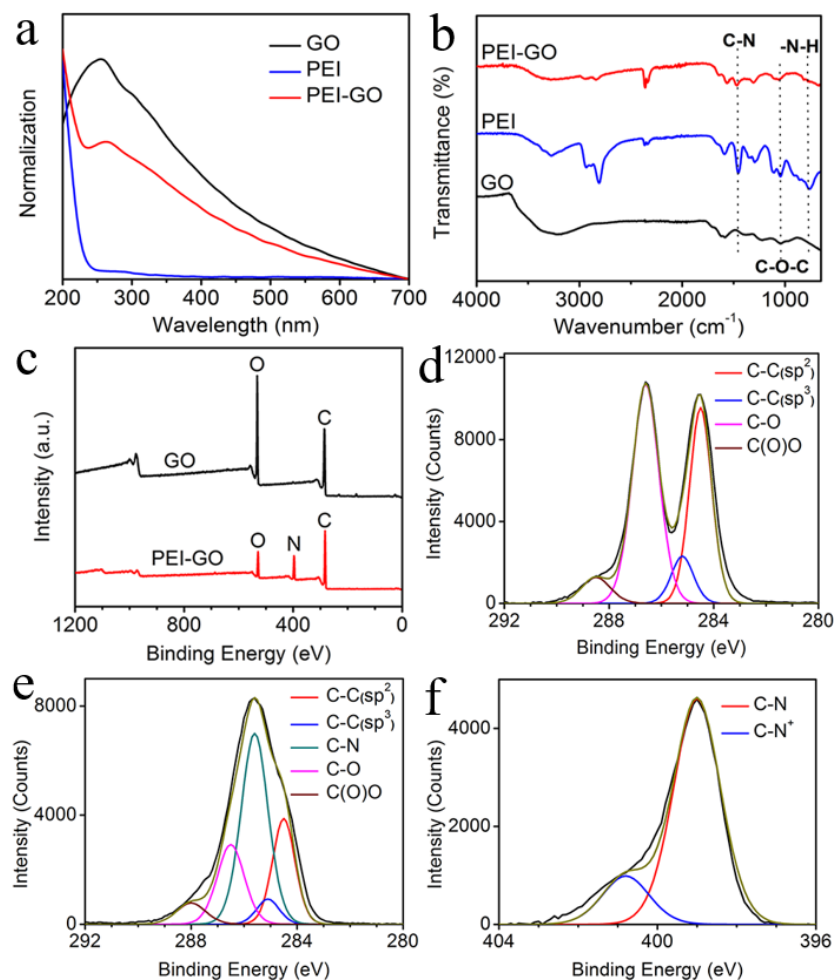


**Figure 2.** (a) UV-*vis* spectra of GO, PEI and PEI-GO. (b) FTIR spectra of GO, PEI and PEI-GO. (c) Full range XPS spectra of GO and PEI-GO. XPS C1s spectra of (d) GO and (e) PEI-GO. (f) XPS N1s spectrum of PEI-GO.

### Bacterial growth inhibition activity of PEI-GO

We further studied the antibacterial activity of PEI-GO using the standard broth dilution method. MIC refers to the lowest concentration of the antibacterial agent that inhibits the visible growth of bacteria after incubating overnight.<sup>41</sup> The turbidity of the culture dishes indicates the amount of bacterial growth, meaning that less turbidity of a dish corresponds to a better antibacterial activity of an agent. We used blank Mueller-Hinton Broth as a control to represent clear solution. Table 1 and Figure S3 show the Broth microdilution MIC results of GO, PEI and

PEI-GO towards both Gram-positive (*e.g. S. aureus*, including MRSA) and Gram-negative (*e.g. E. coli* and carbapenem-resistant *E. coli*, CRA) bacteria. GO and PEI have little effect on the tested bacteria (Table 1). The *S. aureus* and *E. coli* bacteria culture dishes treated with GO at different concentrations present as turbid compared to the control one (Figures S3). On the contrary, PEI-GO exhibits inhibition of bacterial growth on Gram-positive bacteria with MIC of 8  $\mu\text{g/mL}$  (Table 1). The photos show that PEI-GO treated *S. aureus* bacteria culture dishes are clear (Figure S3). The bacterial growth inhibition activity of PEI-GO is due to the coexistence of PEI and GO. However, the solutions of *E. coli* treated with PEI-GO stayed turbid (Figure S3), illustrating PEI-GO is less effective to Gram-negative bacteria. The different performances of PEI-GO towards various bacteria are related to the bacterial structures. The outer membrane presented in Gram-negative bacteria forms a permeability barrier against substances and macromolecules,<sup>42</sup> making higher resistance to antibacterial agents.

**Table 1.** MIC test of PEI-GO on *S. aureus* and *E. coli*

Sample	MIC ( $\mu\text{g/mL}$ )			
	Gram-positive bacteria		Gram-negative bacteria	
	<i>S. aureus</i>	MRSA	<i>E. coli</i>	CRE
GO	>128	>128	>128	>128
PEI	>128	>128	>128	>128
PEI-GO	8	8	>128	>128

### **Antibacterial activity of PEI-GO**

We further investigated the antibacterial property of the PEI-GO towards *S. aureus* (ATCC 29213) using time-kill assay, which reflects the killing rate of bacteria by PEI-GO. Figure 3a shows the viability of *S. aureus* as a function of incubation time with the PEI-GO at different concentrations. PEI-GO shows a faster killing rate at higher concentration: at eight times of the MIC, *S. aureus* is almost killed after 4 h. The time is reduced to 2 h if 16 times of the MIC is used. Table S2 summarizes the antibacterial activity of various carbon nanomaterials in suspension. Previous literature mainly focused on the carbon nanomaterials against Gram-negative strains such as *E. coli* while Gram-positive strains were rarely investigated. PEI-GO shows a higher efficiency in killing the bacteria among the reports, which could completely kill *S. aureus* under the concentration of 64  $\mu\text{g/mL}$  in 4 h.

### **Cell-membrane permeability of PEI-GO**

SYTOX Green assay was performed to assess the bacteria cell membrane disruption potential of PEI-GO. SYTOX Green has a high affinity to nucleic acid. It can easily penetrate the damaged membrane and fluorescence the dead cells with bright green but not cross the membrane of the living cells.<sup>43</sup> With the addition of PEI-GO to *S. aureus*, the fluorescence intensity of SYTOX Green exhibits a concentration-dependent increase (Figures 3b and S4), indicating that the antibacterial activity of PEI-GO is enhanced with the concentration increased. We also used daptomycin as a positive contrast since it is a widely used anti-Gram-positive bacterial agent that seriously disrupts the bacterial cytoplasmic membrane.<sup>44-47</sup> The fluorescence intensity of PEI-GO at concentration of 64  $\mu\text{g/mL}$  is comparable to daptomycin at concentration of 16  $\mu\text{g/mL}$ , indicating the high antibacterial performance of PEI-GO.

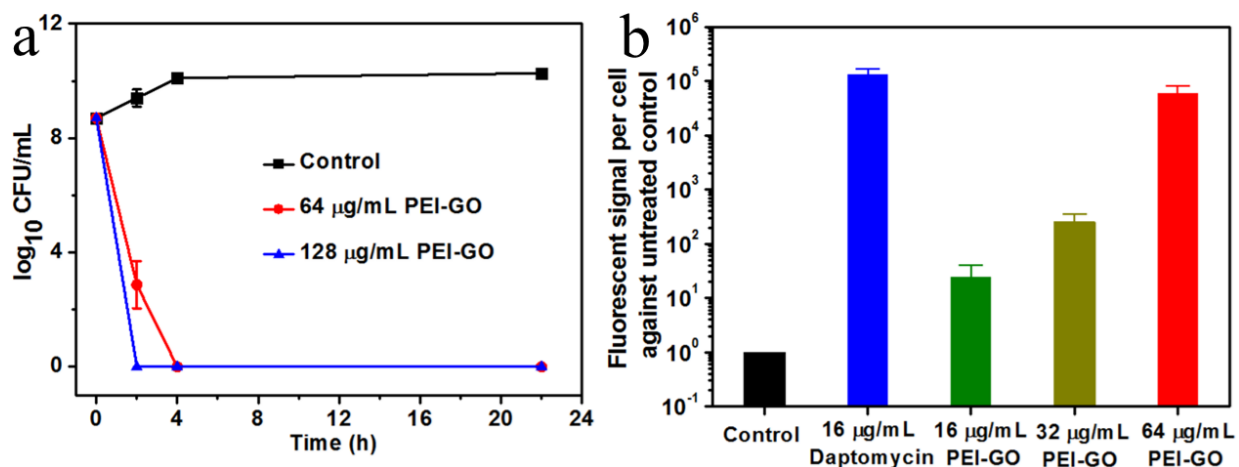


**Figure 3.** (a) Time-kill curves of *S. aureus* (ATCC 29213) treated with different concentrations of PEI-GO. The surviving bacteria were plated at various time points. (b) Cell-membrane permeability effects of the daptomycin and PEI-GO detected by the SYTOX Green assay. Fluorescence signals are directly proportional to the permeability.

### Synergistic effect between PEI-GO and daptomycin

We further find the synergistic effect between PEI-GO and daptomycin in anti-Gram-positive bacterial activity. Three Gram-positive *S. aureus* including MRSA 1114 strain and *S. aureus* ATCC29213, ATCC1717 strains were chosen for the MIC tests. As shown in Figure 4, the MICs of daptomycin against the three bacterial strains are respectively 2, 0.25 and 0.25  $\mu$ g/mL. After combining daptomycin with PEI-GO in different concentrations, the MIC is reduced. The PEI-GO with the concentration of 2-4  $\mu$ g/mL reduced the MIC by 2-fold for MRSA and 4-fold for *S. aureus*. Most importantly, when employing PEI-GO at 1-2  $\mu$ g/mL, the MIC against MRSA decreased from 2 to 1  $\mu$ g/mL, indicating that PEI-GO has a synergistic effect with daptomycin to resensitize daptomycin-resistant MRSA (MIC > 1  $\mu$ g/mL). The synergistic effect between PEI-GO and daptomycin provides promising hopes for reducing the development of daptomycin resistance and increasing bacteria killing power as compared with daptomycin monotherapy.

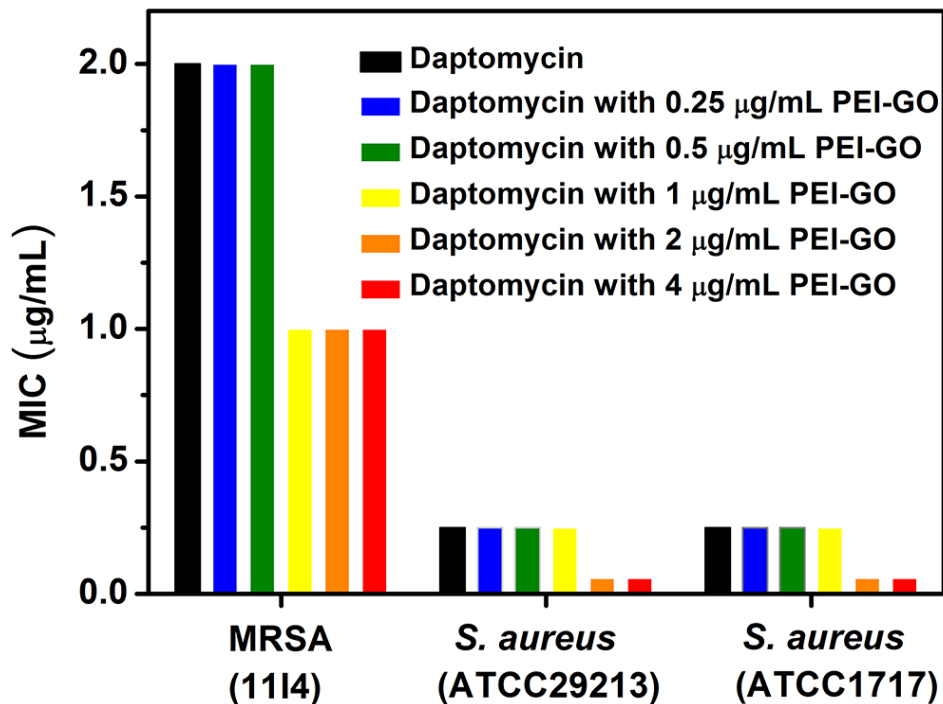
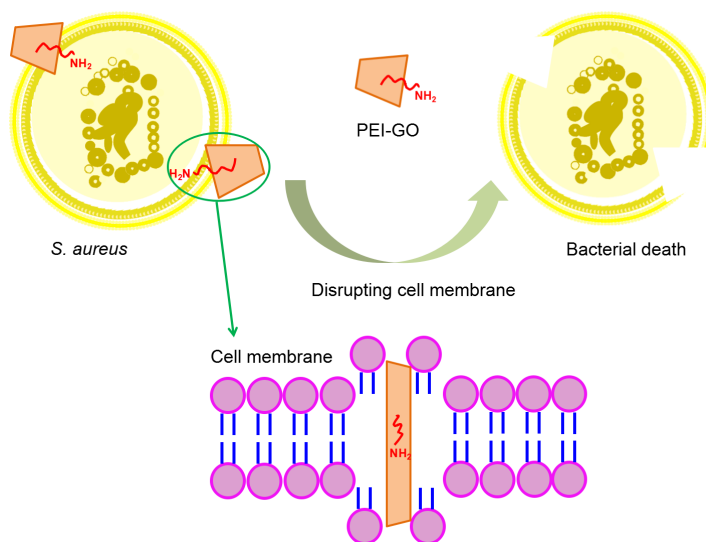


**Figure 4.** MIC test of daptomycin, daptomycin combined with PEI-GO on *S. aureus* with three different strains (11I4, ATCC29213 and ATCC1717).

### Possible antibacterial mechanism

We then explain the possible anti-Gram-positive bacterial mechanism of PEI-GO. The antibacterial activity of the PEI-GO could be attributed to the damaged membrane caused by the sharp edge and chain structure of the PEI-GO nanosheets as well as the high-density amine groups presented in the PEI chains as shown in Scheme 2. The MIC test of the GO, PEI and PEI-GO revealed that the GO and PEI showed negligible antibacterial effect, while the PEI-GO exhibited improved bacteria growth inhibition (Table 1). It has been reported that nanosheets could serve as “cutters” to damage the membrane.<sup>23,48</sup> As a polymer, individual PEI in aqueous solution tends to form random-coil configuration.<sup>49</sup> After the modification of PEI on GO, PEI grafted uniformly on GO and formed chain structure, which led to the disturbance of the bacteria

cell membrane. As verified by AFM (Figure 1), the thickness of the PEI-GO was reduced by 50% as compared with the pristine GO, which increased the sharpness of the edge, making PEI-GO easier to interact with the membrane. In addition, the COOH group on the pristine GO and the newly formed OH group on the PEI-GO surface could supply hydrogen ions to protonate the amine groups on PEI. The protonated amine groups, which was confirmed by the XPS N1s spectrum (Figure 2f), on the PEI have a relative high binding affinity to the negative charged bacteria cell membrane.<sup>50-53</sup> Thus, the protonated amine groups attach to the membrane of the bacteria, inducing the sharp edge and chain structure in nanosheets to damage the membrane, which leads to the release of intracellular ingredients and bacterial death. Since daptomycin can insert into and damage the cell membrane, the addition of the PEI-GO into daptomycin promotes this process and reduces the dosage of daptomycin for killing bacteria.



**Scheme 2.** Schematic illustration of possible antibacterial mechanism of PEI-GO.

## CONCLUSIONS

We have prepared stable aqueous dispersion of PEI-GO *via* a one-step synthesis through the epoxy ring opening reaction and demonstrated its antibacterial activity. MIC test results show



that PEI-GO exhibits a significant bacterial growth inhibition activity towards Gram-positive bacteria with MIC as low as 8  $\mu\text{g}/\text{mL}$ . Furthermore, time-kill curves assay shows the bacterial killing ability of PEI-GO. SYTOX Green assay illustrates the bacteria cell membrane permeability of PEI-GO. Most importantly, the PEI-GO with the concentration of 1-2  $\mu\text{g}/\text{mL}$  shows synergistic effect with daptomycin to resensitize daptomycin-resistant MRSA. Synergistic effect between PEI-GO and daptomycin provides a possible way to increase bacterial killing and reduce the development of daptomycin resistance. PEI-GO with the desirable antibacterial activity has great potential for clinical pathogenic bacteria treatment. Although a detailed antibacterial mechanism study of PEI-GO is required in the future work, the bactericidal activity has been realized by our selection strategy of modifier, which is applicable to other carbon nanomaterials.

## ASSOCIATED CONTENT

### **Supporting Information.**

Photographs of GO and PEI-GO aqueous dispersions (Figure S1). XRD patterns and Raman spectra of GO and PEI-GO (Figure S2). XPS surface chemical composition of GO and PEI-GO (Table S1). Photographs of GO and PEI-GO for MIC test (Figure S3). Comparison of antibacterial activity studies of carbon nanomaterials in suspension (Table S2). Microscopic and fluorescent images of SYTOX Green assay (Figure S4).

## AUTHOR INFORMATION

### **Corresponding Author**

\*Email: [apsplau@polyu.edu.hk](mailto:apsplau@polyu.edu.hk)

## Author Contributions

S.P.L. and Z.F. conceived the idea. Z.F. and K.K.W. prepared and characterized the materials. Z.F., H.L.P. and S.C. contributed to the MIC, time-kill curves assay and SYTOX Green assay experiments. S.P.L., S.C., Z.F. and H.L.P. co-wrote the paper, and all the authors commented on the manuscript.

## Notes

The authors declare no competing financial interest.

## ACKNOWLEDGMENT

This work was supported by the Research Grants Council (RGC) of Hong Kong (Project No. PolyU 153012/14P) and PolyU grants (1-ZVGH and 1-BBAD).

## REFERENCES

1. LeClerc, J. E.; Li, B.; Payne, W. L.; Cebula, T. A., High Mutation Frequencies among *Escherichia Coli* and *Salmonella* Pathogens. *Science* **1996**, *274*, 1208-1211.
2. Levy, S. B.; Marshall, B., Antibacterial Resistance Worldwide: Causes, Challenges and Responses. *Nat. Med.* **2004**, *10*, S122-S129.
3. Magiorakos, A. P.; Srinivasan, A.; Carey, R.; Carmeli, Y.; Falagas, M.; Giske, C.; Harbarth, S.; Hindler, J.; Kahlmeter, G.; Olsson-Liljequist, B., Multidrug-Resistant, Extensively Drug-Resistant and Pandrug-Resistant Bacteria: An International Expert Proposal for Interim Standard Definitions for Acquired Resistance. *Clin. Microbiol. Infec.* **2012**, *18*, 268-281.
4. Webb, G. F.; D'Agata, E. M.; Magal, P.; Ruan, S., A Model of Antibiotic-Resistant Bacterial Epidemics in Hospitals. *P. Natl. Acad. Sci. USA.* **2005**, *102*, 13343-13348.

5. Organization, W. H., The Drug-Resistant Bacteria that Pose the Greatest Health Threats. *Nature* **2017**, *543*, 15.
6. Barry, A. L.; Fuchs, P. C.; Brown, S. D., In Vitro Activities of Daptomycin against 2,789 Clinical Isolates from 11 North American Medical Centers. *Antimicrob. Agents Ch.* **2001**, *45*, 1919-1922.
7. Carpenter, C. F.; Chambers, H. F., Daptomycin: Another Novel Agent for Treating Infections Due to Drug-Resistant Gram-Positive Pathogens. *Clin. Infect. Dis.* **2004**, *38*, 994-1000.
8. Critchley, I. A.; Blosser-Middleton, R. S.; Jones, M. E.; Thornsberry, C.; Sahn, D. F.; Karlowsky, J. A., Baseline Study to Determine in Vitro Activities of Daptomycin against Gram-Positive Pathogens Isolated in the United States in 2000-2001. *Antimicrob. Agents Ch.* **2003**, *47*, 1689-1693.
9. Steenbergen, J. N.; Alder, J.; Thorne, G. M.; Tally, F. P., Daptomycin: A Lipopeptide Antibiotic for the Treatment of Serious Gram-Positive Infections. *J. Antimicrob. Chemother.* **2005**, *55*, 283-288.
10. Boucher, H. W.; Sakoulas, G., Perspectives on Daptomycin Resistance, with Emphasis on Resistance in *Staphylococcus Aureus*. *Clin. Infect. Dis.* **2007**, *45*, 601-608.
11. Hayden, M. K.; Rezai, K.; Hayes, R. A.; Lolans, K.; Quinn, J. P.; Weinstein, R. A., Development of Daptomycin Resistance in Vivo in Methicillin-Resistant *Staphylococcus Aureus*. *J. Clin. Microbiol.* **2005**, *43*, 5285-5287.
12. Skiest, D. J., Treatment Failure Resulting from Resistance of *Staphylococcus Aureus* to Daptomycin. *J. Clin. Microbiol.* **2006**, *44*, 655-656.
13. Yang, S. J.; Xiong, Y. Q.; Boyle-Vavra, S.; Daum, R.; Jones, T.; Bayer, A. S., Daptomycin-Oxacillin Combinations in Treatment of Experimental Endocarditis Caused by Daptomycin-

Nonsusceptible Strains of Methicillin-Resistant Staphylococcus Aureus with Evolving Oxacillin Susceptibility (the “Seesaw Effect”). *Antimicrob. Agents Ch.* **2010**, *54*, 3161-3169.

14. Berti, A. D.; Wergin, J. E.; Girdaukas, G. G.; Hetzel, S. J.; Sakoulas, G.; Rose, W. E., Altering the Proclivity towards Daptomycin Resistance in Methicillin-Resistant Staphylococcus Aureus Using Combinations with Other Antibiotics. *Antimicrob. Agents Ch.* **2012**, *56*, 5046-5053.

15. Lingscheid, T.; Poepl, W.; Bernitzky, D.; Veletzky, L.; Kussmann, M.; Plasenzotti, R.; Burgmann, H., Daptomycin plus Fosfomycin, A Synergistic Combination in Experimental Implant-Associated Osteomyelitis Due to Methicillin-Resistant Staphylococcus Aureus in Rats. *Antimicrob. Agents Ch.* **2015**, *59*, 859-863.

16. Zheng, K.; Setyawati, M. I.; Lim, T. P.; Leong, D. T.; Xie, J., Antimicrobial Cluster Bombs: silver nanoclusters packed with daptomycin. *ACS Nano* **2016**, *10*, 7934-7942.

17. Liu, S.; Wei, L.; Hao, L.; Fang, N.; Chang, M. W.; Xu, R.; Yang, Y.; Chen, Y., Sharper and Faster “Nano Darts” Kill More Bacteria: A Study of Antibacterial Activity of Individually Dispersed Pristine Single-Walled Carbon Nanotube. *ACS Nano* **2009**, *3*, 3891-3902.

18. Kang, S.; Pinault, M.; Pfefferle, L. D.; Elimelech, M., Single-Walled Carbon Nanotubes Exhibit Strong Antimicrobial Activity. *Langmuir* **2007**, *23*, 8670-8673.

19. Hu, W.; Peng, C.; Luo, W.; Lv, M.; Li, X.; Li, D.; Huang, Q.; Fan, C., Graphene-Based Antibacterial Paper. *ACS Nano* **2010**, *4*, 4317-4323.

20. Akhavan, O.; Ghaderi, E., Toxicity of Graphene and Graphene Oxide Nanowalls against Bacteria. *ACS Nano* **2010**, *4*, 5731-5736.

21. Perreault, F.; De Faria, A. F.; Nejati, S.; Elimelech, M., Antimicrobial Properties of Graphene Oxide Nanosheets: Why Size Matters. *ACS Nano* **2015**, *9*, 7226-7236.

22. Vecitis, C. D.; Zodrow, K. R.; Kang, S.; Elimelech, M., Electronic-Structure-Dependent Bacterial Cytotoxicity of Single-Walled Carbon Nanotubes. *ACS Nano* **2010**, *4*, 5471-5479.
23. Liu, S.; Zeng, T. H.; Hofmann, M.; Burcombe, E.; Wei, J.; Jiang, R.; Kong, J.; Chen, Y., Antibacterial Activity of Graphite, Graphite Oxide, Graphene Oxide, and Reduced Graphene Oxide: Membrane and Oxidative Stress. *ACS Nano* **2011**, *5*, 6971-6980.
24. Pham, V. T.; Truong, V. K.; Quinn, M. D.; Notley, S. M.; Guo, Y.; Baulin, V. A.; Al Kobaisi, M.; Crawford, R. J.; Ivanova, E. P., Graphene Induces Formation of Pores that Kill Spherical and Rod-Shaped Bacteria. *ACS Nano* **2015**, *9*, 8458-8467.
25. Georgakilas, V.; Otyepka, M.; Bourlinos, A. B.; Chandra, V.; Kim, N.; Kemp, K. C.; Hobza, P.; Zboril, R.; Kim, K. S., Functionalization of Graphene: Covalent and Non-Covalent Approaches, Derivatives and Applications. *Chem. Rev.* **2012**, *112*, 6156-6214.
26. Lonkar, S. P.; Deshmukh, Y. S.; Abdala, A. A., Recent Advances in Chemical Modifications of Graphene. *Nano Res.* **2015**, *8*, 1039-1074.
27. Xie, W.; Weng, L. T.; Chan, C. K.; Yeung, K. L.; Chan, C. M., Reactions of SO<sub>2</sub> and NH<sub>3</sub> with Epoxy Groups on the Surface of Graphite Oxide Powder. *Phys. Chem. Chem. Phys.* **2018**, *20*, 6431-6439.
28. Vicennati, P.; Giuliano, A.; Ortaggi, G.; Masotti, A., Polyethylenimine in Medicinal Chemistry. *Curr. Med. Chem.* **2008**, *15*, 2826-2839.
29. Helander, I. M.; Latva-Kala, K.; Lounatmaa, K., Permeabilizing Action of Polyethyleneimine on Salmonella Typhimurium Involves Disruption of the Outer Membrane and Interactions with Lipopolysaccharide. *Microbiology* **1998**, *144*, 385-390.

30. Khalil, H.; Chen, T.; Riffon, R.; Wang, R.; Wang, Z., Synergy Between Polyethylenimine and Different Families of Antibiotics against A Resistant Clinical Isolate of *Pseudomonas Aeruginosa*. *Antimicrob. Agents Ch.* **2008**, *52*, 1635-1641.
31. Park, S.; Dikin, D. A.; Nguyen, S. T.; Ruoff, R. S., Graphene Oxide Sheets Chemically Cross-Linked by Polyallylamine. *J. Phys. Chem. C* **2009**, *113*, 15801-15804.
32. Huang, T.; Zhang, L.; Chen, H.; Gao, C., A Cross-Linking Graphene Oxide-Polyethyleneimine Hybrid Film Containing Ciprofloxacin: One-Step Preparation, Controlled Drug Release and Antibacterial Performance. *J. Mater. Chem. B* **2015**, *3*, 1605-1611.
33. Tang, X. Z.; Mu, C.; Zhu, W.; Yan, X.; Hu, X.; Yang, J., Flexible Polyurethane Composites Prepared by Incorporation of Polyethylenimine-Modified Slightly Reduced Graphene Oxide. *Carbon* **2016**, *98*, 432-440.
34. Marcano, D. C.; Kosynkin, D. V.; Berlin, J. M.; Sinitskii, A.; Sun, Z.; Slesarev, A.; Alemany, L. B.; Lu, W.; Tour, J. M., Improved Synthesis of Graphene Oxide. *ACS Nano* **2010**, *4*, 4806-4814.
35. Poh, H. L.; Šaněk, F.; Ambrosi, A.; Zhao, G.; Sofer, Z.; Pumera, M., Graphenes Prepared by Staudenmaier, Hofmann and Hummers Methods with Consequent Thermal Exfoliation Exhibit very Different Electrochemical Properties. *Nanoscale* **2012**, *4*, 3515-3522.
36. Ling, L. L.; Schneider, T.; Peoples, A. J.; Spoering, A. L.; Engels, I.; Conlon, B. P.; Mueller, A.; Schäberle, T. F.; Hughes, D. E.; Epstein, S., A New Antibiotic Kills Pathogens without Detectable Resistance. *Nature* **2015**, *517*, 455-459.
37. CLSI, Methods for Dilution Antimicrobial Susceptibility Tests for Bacteria That Grow Aerobically; Approved Standard-Ninth Edition. Methods for Dilution Antimicrobial

Susceptibility Tests for Bacteria That Grow Aerobically. *Approved Standard -Ninth Edition* **2012**.

38. CLSI, Performance Standards for Antimicrobial Susceptibility Testing; Twenty-Sixth Informational Supplement. *CLSI Document M100-S26, Wayne, Pa: CLSI*. **2016**.

39. Kyotani, T.; Moriyama, H.; Tomita, A., High Temperature Treatment of Polyfurfuryl Alcohol/Graphite Oxide Intercalation Compound. *Carbon* **1997**, *35*, 1185-1187.

40. Bai, H.; Li, C.; Wang, X.; Shi, G., On the Gelation of Graphene Oxide. *J. Phys. Chem. C* **2011**, *115*, 5545-5551.

41. Andrews, J. M., Determination of Minimum Inhibitory Concentrations. *J. Antimicrob. Chemoth.* **2001**, *48*, 5-16.

42. Delcour, A. H., Outer Membrane Permeability and Antibiotic Resistance. *BBA-Proteins Proteom.* **2009**, *1794*, 808-816.

43. Roth, B. L.; Poot, M.; Yue, S. T.; Millard, P. J., Bacterial Viability and Antibiotic Susceptibility Testing with SYTOX Green Nucleic Acid Stain. *Appl. Environ. Microb.* **1997**, *63*, 2421-31.

44. Allen, N.; Hobbs, J.; Alborn, W., Inhibition of Peptidoglycan Biosynthesis in Gram-Positive Bacteria by LY146032. *Antimicrob. Agents Ch.* **1987**, *31*, 1093-1099.

45. Alborn, W.; Allen, N.; Preston, D., Daptomycin Disrupts Membrane Potential in Growing Staphylococcus Aureus. *Antimicrob. Agents Ch.* **1991**, *35*, 2282-2287.

46. Silverman, J. A.; Perlmutter, N. G.; Shapiro, H. M., Correlation of Daptomycin Bactericidal Activity and Membrane Depolarization in Staphylococcus Aureus. *Antimicrob. Agents Ch.* **2003**, *47*, 2538-2544.

47. Hobbs, J. K.; Miller, K.; O'Neill, A. J.; Chopra, I., Consequences of Daptomycin-Mediated Membrane Damage in *Staphylococcus Aureus*. *J. Antimicrob. Chemoth.* **2008**, *62*, 1003-1008.
48. Lu, X.; Feng, X.; Werber, J. R.; Chu, C.; Zucker, I.; Kim, J. H.; Osuji, C. O.; Elimelech, M., Enhanced Antibacterial Activity through the Controlled Alignment of Graphene Oxide Nanosheets. *PNAS.* **2017**, *114*, E9793-E9081.
49. Beu, T. A.; Farcaş, A., Structure and Dynamics of Solvated Polyethylenimine Chains. *AIP Conf. Proc.* **2017**, *1916*, 020001-020006.
50. Hsu, S. H.; Tseng, H. J.; Hung, H. S.; Wang, M. C.; Hung, C. H.; Li, P. R.; Lin, J. J., Antimicrobial Activities and Cellular Responses to Natural Silicate Clays and Derivatives Modified by Cationic Alkylamine Salts. *ACS Appl. Mater. Interfaces* **2009**, *1*, 2556-2564.
51. Palermo, E. F.; Lee, D. K.; Ramamoorthy, A.; Kuroda, K., The Role of Cationic Group Structure in Membrane Binding and Disruption by Amphiphilic Copolymers. *J. Phys. Chem. B* **2011**, *115*, 366-375.
52. Carmona-Ribeiro, A. M.; de Melo Carrasco, L. D., Cationic Antimicrobial Polymers and Their Assemblies. *Int. J. Mol. Sci.* **2013**, *14*, 9906-9946.
53. Larraza, I.; Peinado, C.; Abrusci, C.; Catalina, F.; Corrales, T., Hyperbranched Polymers as Clay Surface Modifiers for UV-Cured Nanocomposites with Antimicrobial Activity. *J. Photoch. Photobio. A* **2011**, *224*, 46-54.



Table of Contents graphic.

